The fate of acylated anthocyanins in mildly heated neutral solution

Julie-Anne Fenger, Rebecca Robbins, Thomas Collins, Olivier Dangles

The fate of acylated anthocyanins in neutral mildly heated solution

Julie-Anne Fenger,[a]* Rebecca J. Robbins,[b] Thomas M. Collins,[c] Olivier Dangles[a]*

[a] *Avignon University, INRA, UMR408, 84000 Avignon, France*
[b] *Mars Wrigley, 1132 W Blackhawk Street, Chicago, IL 60642, USA*
[c] *Retired*

*Corresponding authors.

E-mail addresses: julie-anne.fenger@univ-avignon.fr, olivier.dangles@univ-avignon.fr.

ABSTRACT

In neutral solution, anthocyanins acylated by hydroxycinnamic acids typically exhibit attractive blue colors and a higher resistance to color loss compared to their nonacylated homologs. However, they remain vulnerable to a poorly understood combination of oxidative and hydrolytic reactions that strongly contribute to color loss and limits their industrial applications. In this work, the thermal degradation of isolated red cabbage anthocyanins (0, 1 or 2 acyl groups) at pH 7 was investigated by UPLC-DAD-MS (low- and high-resolution). Non-oxidative alterations, including deacylation and intramolecular acyl transfer, were observed and found very dependent on the number and position of the acyl group(s) as well as on the presence of iron ions. At intermediate and advanced thermal degradation, several oxidative mechanisms were evidenced that lead to protocatechuic acid, phloroglucinaldehyde 2-O-glucoside, acylglycosides and derivatives of 2,4,6-trihydroxyphenylacetic acid and 3,5,7-trihydroxycoumarin. Based on the product distribution observed and on the impact of added Fe^{2+} ions and H_2O_2, possible degradation mechanisms are discussed. They likely start with a one- or two-electron transfer from the anionic base (a major colored form in neutral solution) to O_2. The hydrogen peroxide produced could then further react as an electrophile with the anionic base and/or the hemiketal (major colorless hydrated form).

This contribution to understanding the degradation mechanisms of anthocyanins around neutrality can open up new stabilization strategies to extend the range of their food applications to neutral media.

1. Introduction

Anthocyanins are plant pigments expressing a wide array of red to blue colors depending on pH and the presence of other species susceptible to interact with the anthocyanidin chromophore, such as phenolic compounds (copigments) and metal ions [1]. In particular, anthocyanins and their complexes can express attractive blue colors around neutral pH [2]. This is the case of 3-O-sophorosyl-5-O-glucosylcyanidin and peonidin derivatives commonly found in purple vegetables (*e.g.*, red cabbage) [2–4]. Most importantly, purple vegetables are typically rich in anthocyanins acylated by *p*-hydroxycinnamic acids (HCA), which increase color stability and participate in color diversification. However, at neutral and mildly alkaline pHs, color loss remains relatively fast, which is a serious hurdle to industrial development.

Color loss in anthocyanin solutions at pH > 2 is due to the reversible water addition to the flavylium ion (with concomitant accumulation of a colorless hemiketal and pale yellow *cis*- and *trans*-chalcones) and to a combination of irreversible routes (hydrolytic and oxidative pathways) typically resulting in cleavage of the C-ring [5]. The color stability of diacylated anthocyanins is much higher than for non- or mono-acylated anthocyanins [2,6,7]. Indeed, the HCA residues can develop π-stacking interactions with the anthocyanidin chromophore (intramolecular copigmentation + self-association), thereby protecting it against water addition [1]. By contrast, the rate of irreversible degradation at pH 7 barely depends on the acylation pattern in the case of red cabbage anthocyanins [6]. Indeed, diacylation results in a higher proportion of the colored anionic base at pH 7, which is probably a much better electron donor (thus more vulnerable to autoxidation) than the neutral colorless forms more readily accumulated from the weakly acylated pigments.

The mechanisms of irreversible degradation have been mainly investigated at acidic pH [8–13] and only a few studies were also carried out at neutral pH in the presence of radical initiators, H_2O_2 or ascorbate (a H_2O_2 generator by autoxidation) [14,15]. In the pH range 2 - 4, anthocyanins were reported to be degraded into B-ring + C2 (*e.g.*, protocatechuic acid) and A-ring + C4 (*e.g.*, phloroglucinaldehyde) fragments, C3 being probably eliminated as CO_2. The colorless species, in particular the chalcones, were proposed to be intermediates in the irreversible degradation of anthocyanins at acidic pH [8,13]. At pH 7 – 8, the electrophilic flavylium ion (a diacid with pK_a ~ 4 and 7) is in trace amounts so that water addition is very

77 slow [16]. Anthocyanins are thus mostly a mixture of neutral / anionic bases, with low
78 concentrations of hemiketal and neutral / anionic *cis*- and *trans*-chalcones (pK_a ~ 8) gradually
79 appearing [17].

80 At pH 7, more stable blue colors can be obtained with cyanidin derivatives in the
81 presence of metal ions such as Fe^{2+}, Fe^{3+} and Al^{3+} [18]. Upon metal binding, the
82 anthocyanidin chromophore adopts a *p*-quinonemethide structure, which unlike the flavylium
83 ion does not undergo water addition with concomitant color loss. In spite of this color
84 stabilization, irreversible degradation occurs over a prolonged storage. Addition of Fe^{2+} was
85 reported to be actually protective with diacylated anthocyanins, which strongly bind iron (a
86 possible consequence of the strong π-stacking interactions), but unexpectedly deleterious for
87 the non- and monoacylated homologs, suggesting that iron leakage from the corresponding
88 less stable complexes results in a prooxidant effect [6].

89 Unraveling the degradation mechanisms of anthocyanins around neutrality can open up
90 specific stabilization strategies for anthocyanins used as blue colors. Therefore, this study
91 aims at identifying the main products of irreversible degradation at pH 7. A set of 3
92 anthocyanins from red cabbage (from non- to diacylated) was thermally degraded at neutral
93 pH, 50°C. The role of O_2, added Fe^{2+} and hydrogen peroxide in these mechanisms was
94 investigated. Based on the product distribution observed and on the impact of added Fe^{2+} ions
95 and H_2O_2, possible degradation mechanisms are discussed.

96

97 ## 2. Materials & methods

98 ### *2.1. Materials*

99 Red cabbage anthocyanins were isolated from red cabbage by preparatory LC according
100 to already published procedures [19]. The pigments investigated in this work encompass a
101 nonacylated anthocyanin (PA) and its homologs with a *p*-coumaroyl (pC) residue (P1) and an
102 additional sinapoyl (Sp) residue (P4). PA: cyanidin-3-O-[Glc-2-O-Glc]-5-O-Glc, P1:
103 cyanidin-3-O-[(6-O-pC)-Glc-2-O-Glc]-5-O-Glc, and P4: cyanidin-3-O-[(6-O-pC)-Glc-2-O-
104 (2-O-Sp)-Glc]-5-O-Glc. Stock solutions (5 mM) of pigment were prepared in aqueous 0.01 M
105 HCl (metal-trace grade). Aqueous H_2O_2, $FeSO_4$, $7H_2O$, NaH_2PO_4, $2H_2O$, Na_2HPO_4, $7H_2O$ and

106 the following standards for LC quantification, cyanin (cyanidin-3,5-O-diglucoside), *p*-
107 coumaric acid and sinapic acid, were all obtained from Sigma-Aldrich (St Louis, MO, USA).
108 HPLC-MS grade water was used in all experiments.

109 For each pigment, the fraction of colored and colorless species at equilibrium at pH 7
110 (Scheme 1-SI, Fig. 1-SI) was calculated using the global acidity constant of the flavylium ion
111 (formation of the neutral base + colorless forms) and the two stepwise acidity constants
112 (sequential formation of the neutral and anionic bases) [2].

113 The thermal degradation of anthocyanins was performed at 50°C in a thermostated
114 water bath protected from light, as already described [6]. The initial anthocyanin
115 concentration in the 0.01 M phosphate buffer was $5x10^{-5}$ M. Aliquots were taken up at regular
116 time intervals over 8h and at 24 and 72h. The total concentration in residual pigment was
117 quantified with a UV-Vis spectrophotometer (Agilent 8453) immediately after cooling and
118 acidification to pH 1.0 – 1.5 (fast conversion of the residual colored forms, hemiketal and *cis*-
119 chalcone into the flavylium ion) and 6 to 50h later (additional conversion of the *trans*-
120 chalcone) (Fig. 2-SI).

121 *2.2. Product identification and quantification*

122 The acidified and stabilized samples were analyzed with an Acquity UPLC (Waters
123 Corporation, Milford, USA) equipped with a binary solvent delivery manager and a diode
124 array detector (DAD). Samples (5 µL) were injected onto an Acquity UPLC BEH C18
125 reversed phase column (50x2.1 mm, 1.7 µm) set at 30°C. Phase A (1% HCO_2H in H_2O) and B
126 (1% HCO_2H in MeCN) were eluted at 0.4 mL/min. Unless otherwise specified, all
127 chromatograms are presented at 280 nm after 24h at pH 7, 50°C. Only peaks with S/N > 8 on
128 the 280 nm chromatogram were considered for identification. For P1 and P4, gradient 1 (%B:
129 0 min: 2%, 12 min: 24%, 14-15 min: 80%, 16-18 min: 2%) was used. For PA, gradient 2
130 (%B: 0-2.5 min: 2%, 7 min: 8%, 10 min: 24%, 13 min: 80%, 14-16 min: 2%) enabled a better
131 separation of the more polar degradation products.

132 The UPLC system was coupled with a ESI-Q-trap HCT Ultra (Bruker Daltonics,
133 Bremen, Germany) in ultrascan mode. The capillary voltage was -1.8 kV (positive mode) or
134 2.2 kV (negative mode) with a 80-1500 *m/z* scanning interval at a speed of $26x10^3$ *m/z* s^{-1}.

Desolvation was conducted with N_2 at 365°C, 40 psi, 540 L/h. Cone voltage was 40 V, and the fragmentation amplitude was 1.2 V.

For confirmation of raw formulae, three samples of P1 (t = 0, 24h, 24h in the presence of Fe^{2+}) were also analyzed on a Waters Acquity UPLC system coupled with a Waters Synapt G2-Si High Resolution Mass Spectrometer (HRMS) equipped with an ESI source (Waters Co.). The source and desolvation temperatures were set at 120°C and 500°C, respectively. Desolvation was also conducted with N_2 at 500°C (40 psi) at 800 L h^{-1}. The capillary and cone voltages were set at 0.8 kV and 5 V, respectively. The scan range was *m/z* 50–1500 with a spectrum acquisition every 0.2 s and a resolution of $4x10^4$. Mass scale was corrected during acquisition using leucine enkephalin (Sigma-Aldrich). Data were acquired using the MassLynx™ (V4.2) software in continuum mode. The *m/z* accuracy (Δ, in ppm) of the parent ions was calculated as the relative difference to their expected monoisotopic ion.

Anthocyanin were quantified as cyanin equivalent with a correction factor accounting for the differences in molar absorption coefficient at λ_{max}(Vis) between the pigments [19]. The monoacylsophorose compounds and coumarin derivatives were quantified in HCA equivalent and phloroglucinaldehyde (PGA) derivatives in PGA equivalent.

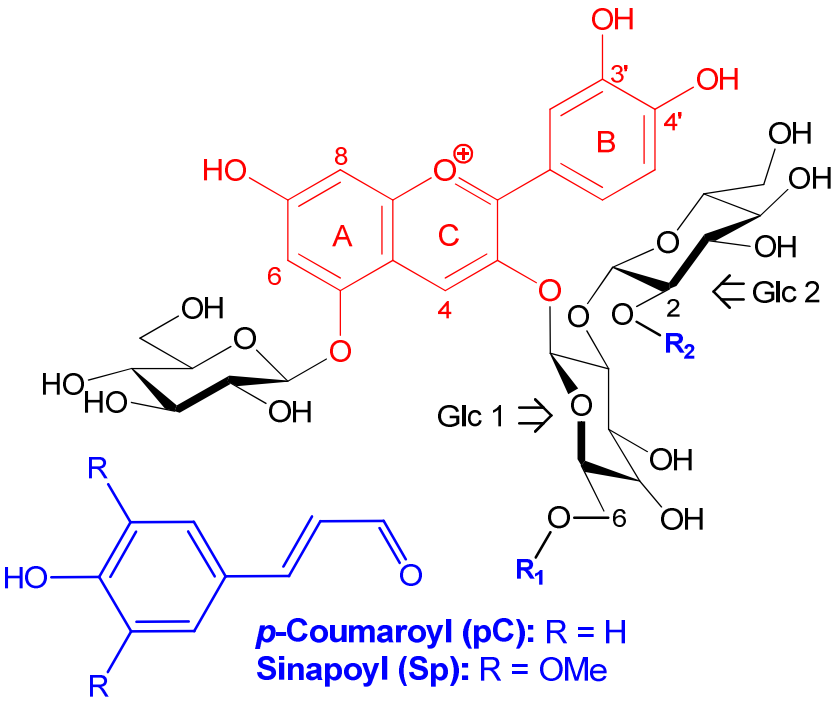

	R1	R2
PA	H	H
PB	H	Sp
P1	pC	H
P4	pC	Sp

Scheme 1. Structures of the red cabbage anthocyanins studied in this work

3. Results

At pH 7 and 50°C, the color stability of diacylated anthocyanin P4 and its iron complex is much higher than that of its non- and mono-acylated counterparts PA and P1 [6]. However, the global color loss is the result of a reversible component featuring water addition to the flavylium ion (and subsequent isomerization steps) and of an irreversible component of true oxidative degradation. The latter component can be appreciated by reversing the former through reacidification to pH 1.0 - 1.5, so as to convert all colored and colorless forms into the flavylium ion. Hence, the time dependence of the residual flavylium percentage solely reflects the rate of oxidative degradation occurring in neutral solution (Fig. 2-SI). After 24h, the percentage of residual flavylium ion lies in the range 40 - 60% and is mostly independent of the acylation pattern. Product identification was then carried out (Fig. 1, Table 1).

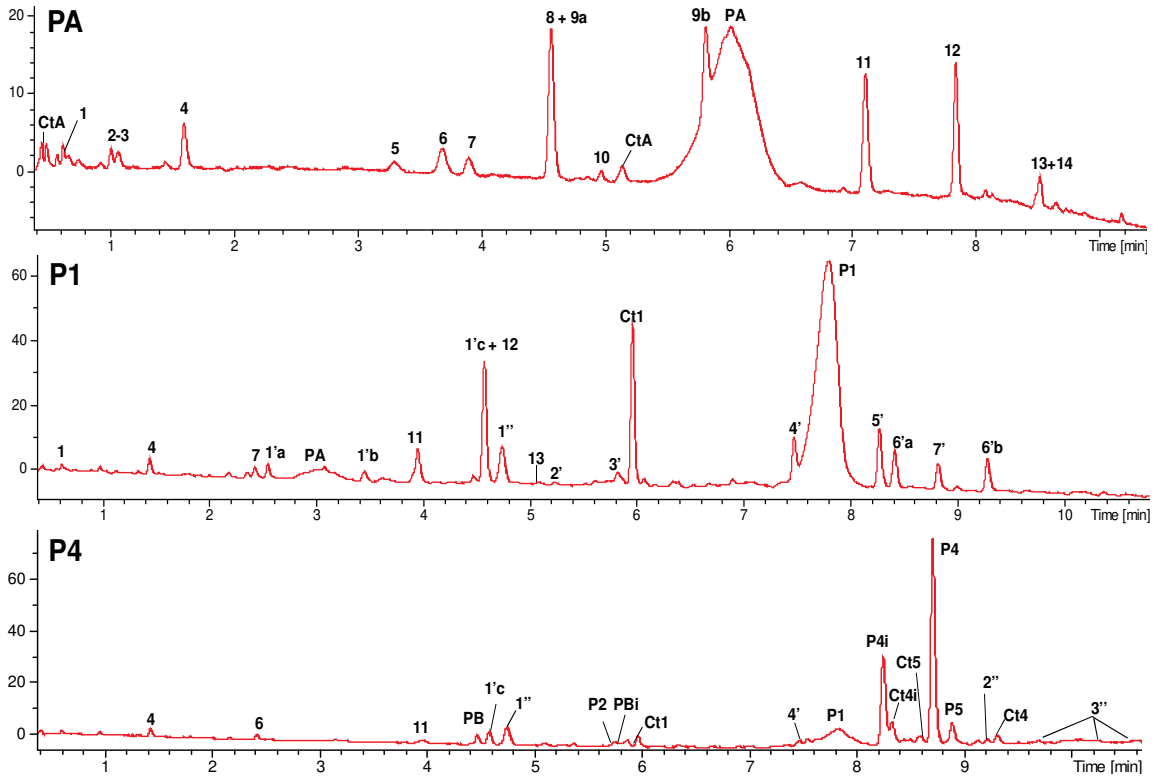

Fig. 1. Chromatograms of the solutions of PA (gradient 2), P1 and P4 (gradient 1) after 24h at pH 7, 50°C (detection at 280 nm). P5 (cyanidin-3-O-[(6-O-Fl)-Glc-2-O-(2-O-Sp)-Glc]-5-O-Glc) is

a contaminant of the P4 sample. Its chalcone (Ct5) and its hydrolysis product P2 (cyanidin-3-O-[(6-O-pC)-Glc-2-O-Glc]-5-O-Glc) are also detected.

Three types of products were distinguished: a) colorless species resulting from reversible water addition (*trans*-chalcones), b) new pigments, *i.e*. isomers and deacylation products (Fig. 2), c) products of oxidative degradation. In addition, the composition of P1 and P4 solutions after degradation over 24h was determined under different conditions: addition of Fe^{2+}, addition of hydrogen peroxide, inert atmosphere. Finally, degradation routes are proposed and discussed.

Table 1. Selection of ions detected in the solutions of PA, P1 and P4 after 24h at pH 7, 50°C. Products numbered according to elution order with the following convention: product *p* potentially present in all 3 samples, product *p*' potentially present in P1 and P4 samples, product *p*" specifically present in P4 samples (see Fig. 1).

#	R_t (min)	Proposal	λ_{max} (nm)	*m/z* (-)	Ion type (-)	MS2 (-)	MS3 (-)
PA: Cya-3-[O-Glc-2-O-Glc]-5-O-Glc (gradient 2)							
1	0.67	C3-Glc	275	345	$[M-H]^-$	345 -> 165 (-Glc-H_2O); 139 (-Glc-CO_2); 183 (-Glc)	-
2-3	1.07	Unid.	291 325	643 1253	$[M+Cl]^-$ $[2M-H]^-$	1253 -> 1055; 1235; 893; 643 -> 527; 617	1055 -> 893; 783; 551 527 -> 445; 783; 365
4	1.60	C2	258	109	$[M-H-CO_2]^-$	-	-
5	3.25	C1-3-Soph -5-Glc	325	715	$[M+Cl]^-$	715 -> 517 (-Cl-Glc); 679 (-Cl)	517 -> 247; 191; 337
6	3.65	C4-Glc	289	315	$[M-H]^-$	315 -> 153 (-Glc)	153 -> 125 (-CO)
7	3.95	Unid.	293	361	-	-	-
8	4.55	C6-Soph	275	529	$[M-H]^-$	529 -> 409, 205 (-Soph)	-
9a	4.55	C7-Soph	278	597	$[M-H]^-$	597 -> 272 (-Soph-H); 417 (-Glc-H_2O); 297; 555 (-CH_2CO)	272 -> 231; 258; 175
10	4.95	Unid.	270 430	757	-	757 -> 551 (-Glc-CO_2); 595 (-Glc); 713 (-CO_2)	551 -> 371 (-Glc-H_2O); 227; 281

9b	5.78	C7-Soph	278	597	$[M-H]^-$	597 -> 272 (-Soph-H); 417 (-Glc-H_2O); 297; 555 (-CH_2CO)	272 -> 231; 258; 175
CtA	5.15	PA Ct	330	789	[M-H]-	789 -> 627; 517; 285	627 -> 285; 517; 241
PA	5.8-6.3	PA	510	807 825	$[M+Cl-H]^-$ Id.+H_2O	807 -> 771; 609 825 -> 789; 627	771 -> 609; 285; 447 789 -> 627; 517; 285; 447
11	7.20	C3-Glc -Soph-C2	269	805	$[M-H]^-$	805 -> 463 (-Soph-H_2O) 651 (-C2-H_2O); 327 (-C2-Soph-H_2O)	463 -> 327 (-C2); 299 (-pC-H_2O); 165 (-C2-Glc)
12	7.88	C3-Glc-C2	ND	481	$[M-H]^-$	481 -> 345 (-C2); 327 (-C2-H_2O); 463 (-H_2O)	345 -> 165 (-Glc-H_2O); 139 (-Glc-CO_2); 183 (-Glc); 327 (-H_2O)
13	8.47	Cya-5-Glc	ND	447	$[M-2H]^-$	447 -> 285 (-Glc)	285 -> 257
14	8.50	C5-Glc	328	463	$[M-H]^-$	463 -> 419; 257; 445	419 -> 213
P1: Cya-3-O-[(6-O-pC)-Glc-2-O-Glc]-5-O-Glc (gradient 1)							
1'a	2.53	pC-Soph	310	487	$[M-H]^-$	487 -> 469 (-H_2O)	469 -> 205; 307 (-Glc); 265
1'b	3.44	pC-Soph	310	487	$[M-H]^-$	487 -> 469 (-H_2O)	469 -> 205; 307 (-Glc); 265
1'c	3.92	pC-Soph	310	487	$[M-H]^-$	487 -> 469 (-H_2O)	469 -> 205; 307 (-Glc); 265
1'd	4.55	pC-Soph	310	487	$[M-H]^-$	487 -> 469 (-H_2O)	469 -> 205; 307 (-Glc); 265
2'	5.21	C1-3-Soph	310	553	$[M+Cl]^-$	553 -> 499 (-Cl-H-H_2O); 517 (-Cl-H)	517 -> 499 (-H_2O); 235; 295; 179
3'	5.80	Unid.	ND	498	-	498 -> 301 (Cya + O); 336; 463 (Cya-Glc + O)	301 -> 165 (-C4 or C2); 257 (-CO_2); 137
Ct1	5.97	P1 Ct	310	935 971	$[M-H]^-$ $[M+Cl]^-$	935 -> 773; 755; 663; 447; 285; 971 -> 935	663 -> 517; 247; 935 -> 773; 755; 663; 285
4'	7.45	C1-3-(pC)Soph-5-Glc	317	825	$[M-H]^-$	825 -> 663 (-Glc)	663 -> 517 (-pC); 247; 191
P1	7.81	P1	524	917	$[M-2H]^-$	917 -> 755 (-Glc)	755 -> 609 (-pC); 339; 284; 309
5'	8.27	C3-	308	951	$[M-H]^-$	951 -> 623 (-C3-Glc);	463 -> 327 (-C2); 301

		(pC)Soph-Glc-C2				463 (-pC-Soph-H_2O)	(-Glc); 165 (-C2-Glc)
6'a	8.40	C7-(pC)Soph	318	743	$[M-H]^-$	743 -> 659; 597 (-pC); 272 (-pC-Soph-H)	659 -> 479 (-Glc-H_2O); 335
7'	8.83	C6-(pC)Soph	ND	675	$[M-H]^-$	675 -> 529 (-pC); 409; 205 (-pC-Soph)	529 -> 511 (-H_2O); 409; 349 (-Glc-H_2O); 205 (-Soph)
6'b	9.30	C7-(pC)Soph	318	743	$[M-H]^-$	743 -> 659; 597 (-pC); 272 (-pC-Soph-H)	659 -> 479 (-Glc-H_2O); 335
P4: Cya-3-O-[(6-O-pC)-Glc-2-O-(2-O-Sp)-Glc]-5-O-Glc (gradient 1)							
PB	4.46	PB	530	1013	$[M+Cl-H]^-$	1013 -> 977 (-Cl); 815 (-Glc)	977 -> 609 (-Glc)
1''	4.76	pC acid	309	119	$[M-H-CO_2]^-$	-	-
P2	5.76	P2 (cont.)	530	983	$[M+Cl-H]^-$	983 -> 947 (-Cl); 785 (-Glc)	947 -> 785 (-Glc)
PBi	5.88	PB isomer	530	1013	$[M+Cl-H]^-$	1013 -> 977 (-Cl); 815 (-Cl-Glc)	977 -> 609 (-Sp-Glc); 339
P4i	8.12	P4 isomer	530	1159 1123	$[M+Cl-H]^-$ $[M-2H]-$	1159 -> 1123 (-Cl) 1123 -> 961 (-Glc)	961 -> 755 (-Sp); 737 (-Sp-H_2O); 285 (Cya)
Ct4	8.34	P4 Ct	320	1141	$[M-H]^-$	1141 -> 977 (-pC-H_2O); 869	977 -> 853; 935 (-Sp); 469; 285 (Cya)
P4	8.71	P4	534	1123	$[M-2H]^-$	1123 -> 961 (-Glc)	961 -> 755 (-Sp); 737 (-Sp-H_2O); 285 (Cya)
P5	8.89	P5 (cont.)	534	1189	$[M+Cl-H]^-$	1189 -> 1153 (-Cl)	1153 -> 991 (-Glc); 785 (-Glc-Sp); 947 (-Sp)
2''	9.19	C1-Glc-(Sp,pC) Soph	ND	1067	$[M+Cl]^-$	1067 -> 1031 (-Cl)	1031 -> 869 (-Glc); 663 (-Glc-Sp); 825 (-Sp); 517 (-Sp-pC-Glc)
Ct4i	9.31	P4 Ct isomer	320	1141	$[M-H]^-$	1141 -> 977 (-pC-H_2O); 869; 855	869 -> 663 (-Sp); 715; 645 (-Sp-H_2O); 503
3''a	10.0	C7-(Sp,pC) Soph	ND	949	$[M-H]^-$	949 -> 865; 931; 782	931 -> 725; 515; 359
3''b	10.6	C7-(Sp,pC) Soph	ND	949	$[M-H]^-$	949 -> 865; 931; 782	865 -> 711; 847; 539
3''c	11.1	C7-(Sp,pC) Soph	ND	949	$[M-H]^-$	949 -> 865; 931; 782	931 -> 545; 739; 311

180

3.1. Hydration and the reversible accumulation of the trans-chalcone

The fractions of colored and colorless species at the hydration equilibrium (Scheme 1-SI, Fig. 1-SI) are strongly dependent on the acylation pattern. From the global (hydration included) and specific (sequential proton transfers) acidity constants of the flavylium ion at 25°C [2] it is estimated that PA is almost colorless at pH 7 (99% hemiketal B + chalcones). By contrast, the fraction of colored forms is higher for P1 (*ca*. 15%) and P4 (*ca*. 80% colored forms, of which 55% anionic base).

In heated samples (50°C), the residual *trans*-chalcone (Ct) can be detected by UPLC-DAD-MS when the analyses are performed rapidly after acidification. Indeed, its conversion into the flavylium ion is strongly retarded by the slow *cis-trans* isomerization. The PA *trans*-chalcone (CtA) was detected with λ_{max} = 330 nm (Fig. 3-SI), close to the malvidin-3,5-diGlc Ct (λ_{max} = 335 nm) [20]. After 1h, the fraction of Ct reaches *ca*. 29% for PA (Fig. 2-SI). By comparison, at pH 6, the Ct fraction accumulated from the triacylated heavenly blue anthocyanin, which has the same glycosidation pattern as the red cabbage pigments, is 32% [17].

3.2. Deacylation and intramolecular acyl transfer

The acyl groups undergo hydrolysis and intramolecular migration (*trans*-esterification) at pH 7 and 8. After 24h at pH 7, the total yield of these anthocyanin derivatives amounts to 7% for P1 and 28% for P4 (Table 2). The hydrolysis of the protecting acyl moieties must reduce the color stability [1].

The λ_{max} values of P1 and P4 in the visible range after a 24h period of heating at pH 7 were shifted by -1 nm and -6 nm respectively, while the λ_{max} of PA remained unchanged. The decrease in λ_{max} is ascribed to deacylation, at a rate corresponding to the fraction of deacylation products (PA, PB, P1). P1 and PB are respectively formed upon loss of the Sp and pC residues (Fig. 2). When P1 and PB are heated separately under the same conditions, 37% PA is formed from PB after 24h, *vs*. only 14% from P1. This suggests that the Sp residue (at C2-OH of Glc-2) is more prone to hydrolysis than the pC residue (at C6-OH of Glc-1). Investigations with sucrose acylated by fatty acids (pH 7 – 10) also concluded that esters of primary alcohols are more resistant to saponification than esters of secondary alcohols [21].

Anthocyanin deacylation was observed previously in red cabbage extracts. Over storage, a decrease in the diacylated anthocyanins was compensated by an increase in the non- and monoacylated ones [22]. The kinetic monitoring shows that PB is formed from P4 over the first 4 hours, and that isomers of both P4 and PB are formed later (Fig. 2).

A

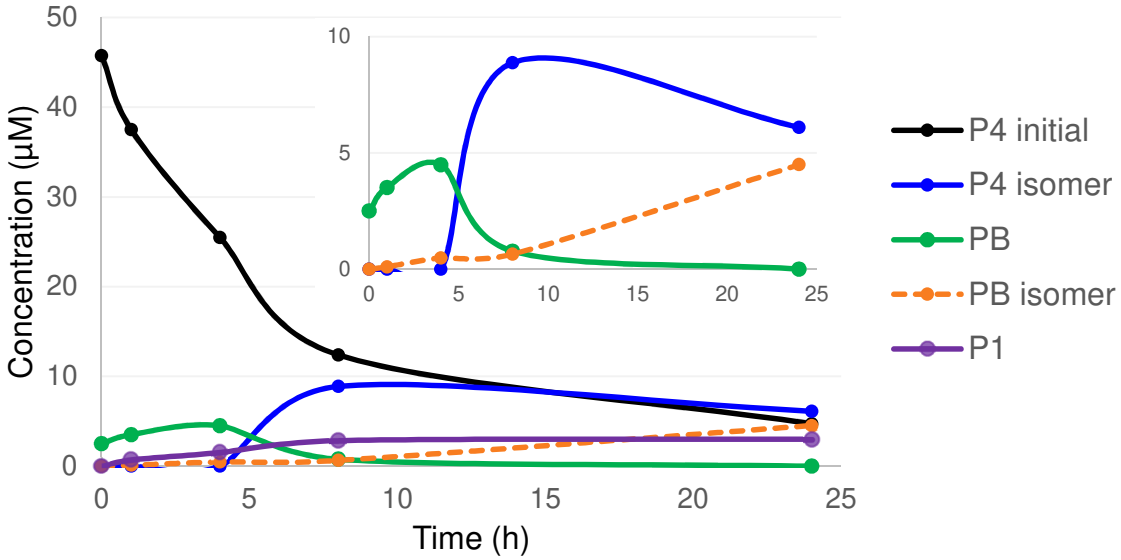

B

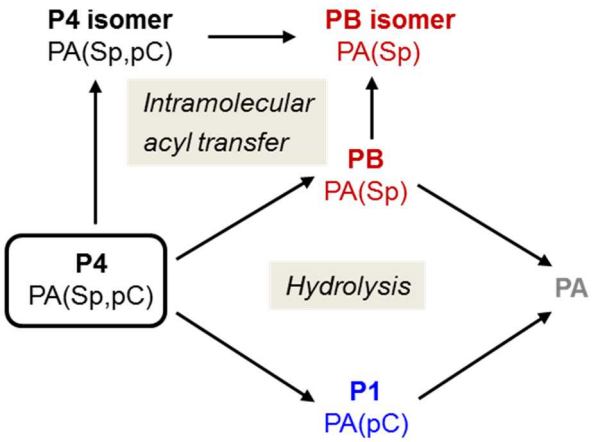

Fig. 2. A: Kinetic monitoring of deacylation and intramolecular acyl transfer for diacylated pigment P4 (pH 7, 50°C, *insert for easier visual appreciation*). The difference between P4 consumption and accumulation of the neoformed pigments is ascribed to oxidative

degradation. **B:** Kinetic scheme and hypothetical intramolecular acyl transfer routes within the sophorose moiety (Glc-2).

Table 2. Quantification by UPLC-DAD of anthocyanin degradation and of the new pigments formed in PA, P1 and P4 solutions after thermal treatment (24h, pH 7, 50°C) in the absence or presence of Fe^{2+}. Concentrations in µM of cyanin equivalent (corrected for differences in molar absorption coefficient between pigments).

	Pigment						**Pigment + Fe^{2+} (0.6 equiv.)**					
	PA		**P1**		**P4**		**PA**		**P1**		**P4**	
	t=0	**t=24h**	**t=0**	**t=24h**	**t=0**	**t=24h**	**t=0**	**t=24h**	**t=0**	**t=24h**	**t=0**	**t=24h**
PA	51.5	12.7	2.5	3.0			51.4	1.5	2.4	0.7		
PB					0.8	1.4					2.3	0.5
P1			54.9	25.4	1.4	3.6			56.5	2.8	3.8	1.1
P1 isomer				0.5								
P4 isomer					0.4	9.1					1.3	0.6
P4					51.7	8.1					53.4	13.5
Total anthocyanins	51.5	12.7	57.4	28.9	54.2	22.2	51.4	1.5	58.9	3.4	60.8	15.7
Acyl loss (%)			4.6	5.2	4.0	8.9			4.3	1.2	10.7	2.6
Acyl transfer (%)				0.6	0.8	16.8					1.4	0.5

Upon heating at pH 7 and 8, a major P4 isomer accumulates (Table 2, Fig. 3-SI). It displays a lower λ_{max} (-4 nm) than P4. Two other isomers are also detected, both remaining very minor. By contrast, P1 isomerization is marginal (< 2%). The hypothesis of *cis-trans* isomerization of the HCA residues can be ruled out, first because the samples were heated in the dark, and second, because it would also have occurred with P1. Hence, the P4 isomers are believed to form upon migration (*trans*-esterification) of a HCA residue within the same Glc. As acyl migration within P1 is negligible, it can be assumed that the labile acyl residue of P4 is the sinapoyl residue at C2'-OH. Similar phenomena were reported for aliphatic esters of sucrose in alkaline aqueous solution [21] with a clear trend of acyl groups to shift from secondary to primary positions. Overall, our data demonstrate that the sinapoyl residue of P4

236 is more sensitive to both hydrolysis and *trans*-esterification than the *p*-coumaroyl residue.

237

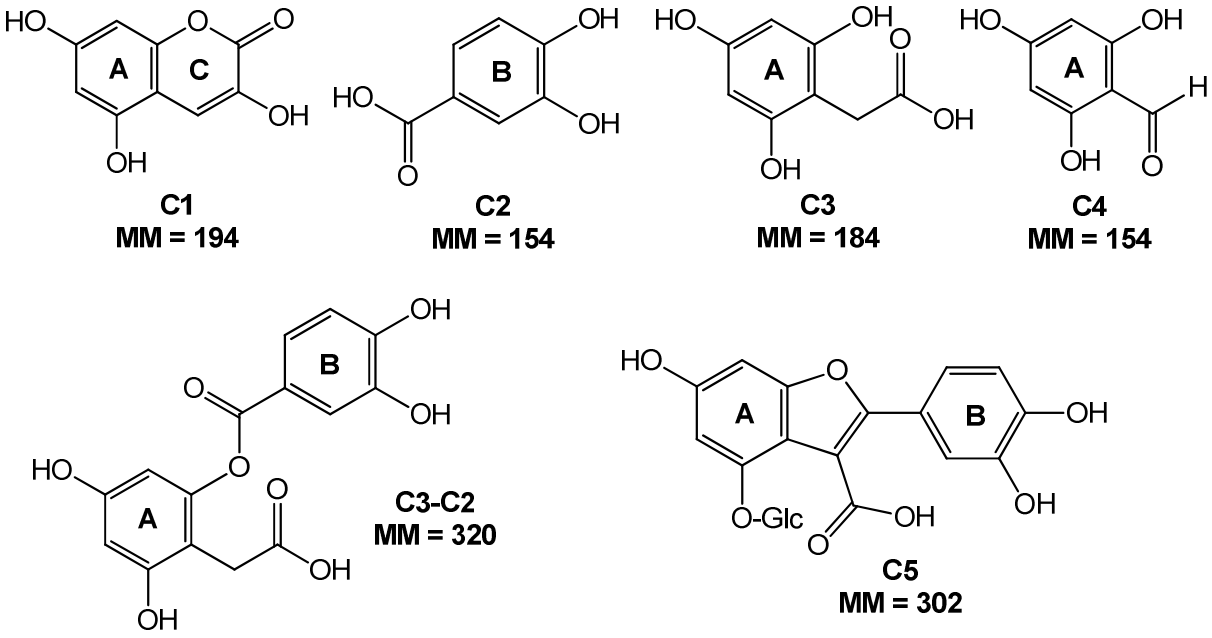

238

239 **Scheme 2.** Proposed core structures for the major compounds detected (see Table 1). C1 =
240 3,5,7-trihydroxycoumarin, C2 = protocatechuic acid, C3 = 2,4,6-trihydroxyphenylacetic acid,
241 C4 = phloroglucinaldehyde. Core structures C6 (MM = 205) and C7 (MM = 274) remain
242 unidentified.

243

244 *3.3. The oxidative products & degradation routes*

245 The products of irreversible degradation of PA, P1 and P4 were characterized by UPLC-
246 MS-DAD (Table 1). Several groups of compounds only differ by the presence of the acyl
247 and/or glucose moieties, and share common fragments in MS^2 and MS^3. In this case, a
248 common core was assumed and tentatively identified (Scheme 2).

249 *3.3.1. Confirmed structures*

250 Compound **4** is detected in PA, P1 and P4 solutions. Its characteristics are identical to
251 those of a commercial standard of protocatechuic acid (noted C2). Besides, C2 formation
252 upon degradation of cyanidin derivatives was reported several times [8,11]. Compound **4** is
253 therefore confidently identified as protocatechuic acid.

Compound **2''** is detected in P4 solution only. The commercial standard of *p*-coumaric acid (pC) displays the same characteristics. In HRMS, the $[M-H]^-$ ion at *m/z* 153.0186 is also detected (calculated value = 153.0203, Δ = 11.1 ppm). Compound **2'',** which is expected from the hydrolysis of P4 into PB, is therefore confidently identified as *p*-coumaric acid.

3.3.2. Probable structures

Compounds **5, 4'** and **2''** were respectively detected in PA, P1 and P4 solutions (Fig. 4-SI). They are thought to be derivatives of 3,5,7-trihydroxycoumarin (noted C1). The λ_{max} of **5** (329 nm) is in agreement with that of the 3,5-O-diglucoside derivative of C1 formed upon treatment of malvidin 3,5-di-O-glucoside (malvin) by H_2O_2 in neutral solution [23]. As for **4'**, its λ_{max} (317 nm) is close to that of free *p*-coumaric acid (310 nm) and in agreement with the reported 3-O-(*p*-coumaroyl)glucoside of C1 (λ_{max} = 315 nm) [23]. In HRMS, **4'** is detected as $[M-H]^-$ at *m/z* 825.2071, in agreement with the calculated monoisotopic value (Δ = 0.6 ppm). Among the fragments identified: the successive losses of Glc to *m/z* 663.1552, and of *p*-coumaroylsophorose down to *m/z* 193.0127. The nonacylated coumarin is also detected from P1 after an extended thermal treatment of 96h. Its raw formula is confirmed by HRMS: *m/z* 715.1473 ($[M+Cl]^-$) and 679.1707 ($[M-H]^-$, Δ = 0.4 ppm). The fragment at *m/z* 553 (from $[M+Cl]^-$) likely results from the loss of Glc at C5-OH. By analogy, **2''** must be the diacylated coumarin C1-3-(pC,Sp)Soph-5-Glc. The following fragments substantiate this hypothesis: 869 ($[M-H-Glc]^-$), 825 ($[M-H-Sp]^-$), 663 ($[M-H-Glc-Sp]^-$) and 517 ($[M-H-Glc-Sp-pC]^-$). Surprisingly, coumarin derivatives were not detected from anthocyanins that are not glycosylated at C5-OH [23]. In the absence of added H_2O_2, these products remain in low amounts (<1% of the initial pigment concentration, Table 1-SI).

A series of compounds having a *m/z* of +34 compared to the native pigments were detected (Fig. 3). The compounds, noted **11**, **12** and **5'**, display similar UV spectra and produce common fragments at *m/z* 463, 345, 327 and 301. Compound **11**, detected from the 3 pigments, is proposed to be C3(Glc,Soph)-C2, an analog of structures formed upon reacting anthocyanins with H_2O_2 [15] or upon their azo-initiated autoxidation [24]. Alternatively, a two-electron oxidized analog was identified in the autoxidation of malvidin 3-O-glucoside in acidic solution [23,25]. From the $[M-H]^-$ ion of compound **12** (C3(Glc)-C2), the loss of C2 and/or H_2O followed by the loss of Glc and/or H_2O or CO_2, was observed (Scheme 2-SI). The *p*-coumaroyl analog of compound **11** (**5'**, *m/z* 951) yields fragments at *m/z* 623 (loss of C3 +

Glc) and 463 (loss of pC + Soph + H_2O). Second fragmentations of the latter ion give fragments with *m/z* 327 (loss of C2), 301 (loss of Glc) and 165 (loss of C2 + Glc). In HRMS, **5'** is detected at *m/z* 951.2348 ($C_{42}H_{48}O_{25}$, Δ = 4.9 ppm). Finally, **12** (*m/z* 481) is identified as C3(Glc)-C2. Overall, these compounds are proposed to be (acyl)glycosides of 2-(3,4-dihydroxy)-benzoyloxy-4,6-dihydroxyphenylacetic acid.

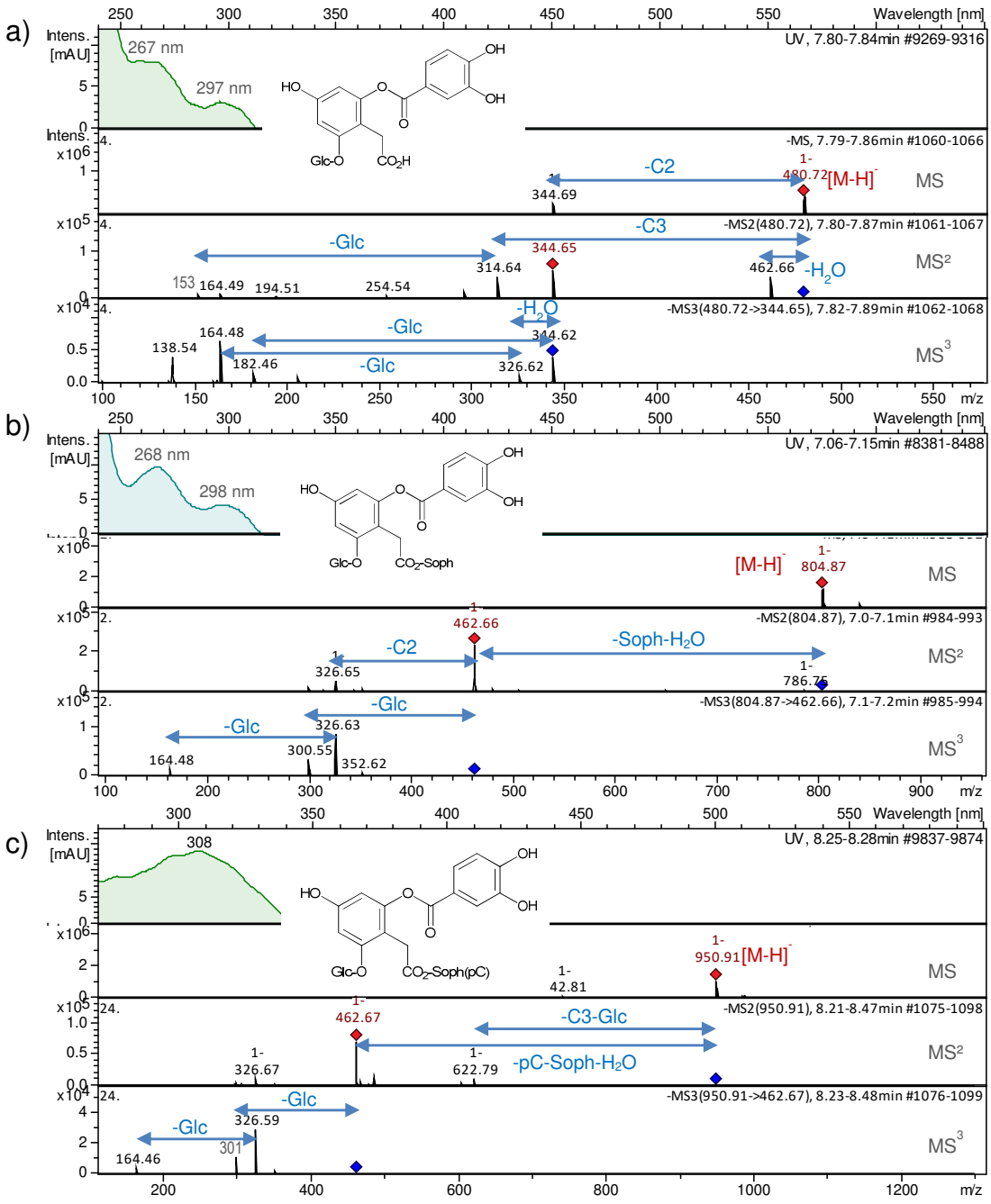

306 **Fig. 3.** UV-visible, MS and MS² spectra of a) C3(Glc)-C2 from PA (**12**, *m/z* 481); b)
307 C3(Soph,Glc)-C2 from PA (**11**, *m/z* 805); c) C3(pCSoph,Glc)-C2 from P1 (**5'**, *m/z* 951).

308

309 Several isomers of compound **1'** (*m/z* 487) were detected from P1 (Fig. 5-SI). The two
310 major ones **1'c** and **1'd** were also detected from P4. They mostly fragment by losing H_2O. In
311 MS3, the additional loss of Glc is observed yielding a fragment ion at *m/z* 307. In ESI(+), ions
312 of *m/z* 511 and 527, respectively corresponding to the Na^+ and K^+ adducts, were detected.
313 Compound **1'** is proposed to be pC-sophorose released by hydrolysis of 1-O-acylglycosides
314 formed during oxidative degradation pathways. Four diacylsophoroses from purple sweet
315 potato anthocyanins were reported and their structures confirmed by NMR [26]. No MS
316 fragmentation data have been reported yet. The pC-sophorose isomers are likely a mixture of
317 regioisomers produced by migration of pC to a neighboring OH group, each potentially
318 present as a mixture of α and β anomers (Fig. 5-SI).

319 As intramolecular acyl migration is negligible for P1, the pC moiety appears labile in
320 the cleavage products only. Thus, it seems that the acyl–cyanidin π-stacking interactions
321 developed by P1 inhibit acyl migration within the sophorose moiety. Only one
322 diacylsophorose (*m/z* 693) in low concentration (< 0.5 µM) could be detected from P4, in
323 agreement to the relatively high sensitivity of the sinapoyl residue to hydrolysis. However,
324 free sinapic acid remains undetected and must be quickly consumed, while free *p*-coumaric
325 acid is detected in P4 solution (Table 1-SI). Consistently, under the same conditions, free
326 sinapic acid undergoes extensive oxidative dimerization after 24h (22% residual content,
327 unpublished data) while *p*-coumaric acid is much more stable (78% residual content).

328 From a 50 µM pigment solution, the pC-sophorose concentration after a 72h heating
329 reached 11.2 µM and 6 µM from P1 and P4, respectively. The concentration did not plateau,
330 suggesting a high stability of these compounds. Overall, acylglycosides come up as useful
331 indicators of the oxidative degradation of acylated anthocyanins in neutral solution.

332 Compound **6** is detected with the 3 pigments. Its main fragment (*m/z* 153) reflects the
333 loss of glucose. The additional loss of 28 (*m/z* 125) is a decarbonylation step expected for
334 aldehydes. A probable structure for **6** is phloroglucinaldehyde 2-O-glucoside. The formula is

in agreement with the detected molecular ion at *m/z* 315.0714 (Δ = 1.0 ppm) and the aglycone at *m/z* 153.0203. Phloroglucinaldehyde and its glucoside were frequently reported as anthocyanin degradation products involving the A-ring [8,11,27]. Compound **6** accounts for *ca.* 10% of all products present at 24h in PA, P1 and P4 solutions (Table 1-SI).

3.3.3. Tentative structures

For the following compounds, no literature data is available. However, the structures proposed are compatible with at least two features among raw formula from high resolution MS, MS2 fragments and UV-visible spectrum.

Compound **1** is detected with the 3 pigments (Fig. 6-SI). The $[M-H]^-$ ion undergoes the loss of Glc but also the concomitant loss of Glc + H_2O, with subsequent decarboxylation. This fragmentation pattern is close to that of C3(Glc)-C2 (**12**, Scheme 2-SI). Based on these characteristics, **1** is proposed to be 2-glucosyloxy-4,6-dihydroxyphenylacetic acid (C3Glc). Compound **1** is probably produced by hydrolysis of the C3-C2 derivatives identified above (**11** and **12**). HRMS confirmed the raw formula proposed for **1**: $C_{14}H_{18}O_{10}$ (*m/z* 345.081, Δ = 1.7 ppm). This group of products is mostly detected from the nonacylated anthocyanin (6.6% of the initial pigment concentration at 24h, Table 1-SI).

3.3.4. Other compounds

Compound **14** is a minor product detected in PA solution. Its fragmentation pattern mainly consists in the loss of CO_2 and water (Fig. 7-SI). A closely related structure (same core noted C5) was reported previously in the reaction of cyanidin 3-O-glucoside with H_2O_2 in a water/ethanol mixture [15]. It is consistent with the raw formula deduced from *m/z* 463.1051 in HRMS (Δ = 1.0 ppm).

Compounds **8** and **7'** are sophorosides of the same unidentified aglycone noted C6 (*m/z* 205.0131, Fig. 8-SI). The chemical formulas of **8** and **7'** are respectively $C_{22}H_{26}O_{15}$ and $C_{32}H_{36}O_{16}$ (Δ = 0.9 and 1.9 ppm).

Similarly, compounds **9**, **6'** and **3"** are sophorosides of the same structure noted C7 (*m/z* 272.0323, even value detected as a fragment with both mass spectrometers, Fig. 9-SI), which has no equivalent in the literature. The raw formula of C7 ($C_{14}H_{10}O_6$) is compatible with the ions detected for **6'** and **9** at the respective *m/z* values of 743.0747 and 597.1446 (Δ = 0.5 and

2.5 ppm). C7 derivatives could be produced by a multistep mechanism starting with the electrophilic addition of H_2O_2 to the anionic base at position C3. Compounds **9**, **6'** and **3"** are all detected as mixtures of 2 or 3 isomers. While acyl transfer can be proposed for **6'** and **3"** to account for this observation, the isomerization of **9** remains unexplained. Moreover, the absence of glucose at C5-OH, which is normally not labile in neutral solution, is surprising. Hence, the structure proposed in Fig. 9-SI must be regarded as tentative.

3.4. Medium effects

The major products - other than anthocyanins - detected after 24h in PA, P1 and P4 are quantified in Table 1-SI. Besides the products of acyl migration, protocatechuic acid (C2) and phloroglucinaldehyde-2-glucoside (C4-Glc) come up as major products. The putative C6 and C7 derivatives are also relatively abundant (*ca.* 10% of the initial pigment concentration).

Fe^{2+} prevents the accumulation of the *trans*-chalcones through the formation of metal complexes resistant to water addition. More surprising is the almost total inhibition of P4 isomerization and deacylation. Higher concentrations of oxidation products, *e.g.* C7 derivatives **6'**, were detected in Fe^{2+}-supplemented P1 solutions (Fig. 10-SI) in agreement with Fe^{2+} promoting P1 autoxidation [6]. This trend is not observed with P4.

Addition of H_2O_2 (1 equiv.) to P1 solution leads to a much higher concentration of pC-sophorose and coumarin derivatives and C3-C2 derivatives (Fig. 3). Addition of H_2O_2 in large excess (10^3 equiv.) induces a fast consumption of the anthocyanin even in the absence of thermal treatment. Under both conditions, pC-sophorose and C1 derivatives are the major products. Moreover, a major, yet unidentified, product (*m/z* 625 and 312, fragment at 183 corresponding to C3) is specifically formed (Fig. 11-SI).

Under argon atmosphere (low O_2 level), more residual pigment is present after 24h and the known oxidation products of P1 and PA are very minor (Fig. 4).

Finally, in order to identify late degradation products of anthocyanins, the heating period was extended to 72h. The chromatograms (Fig. 12-SI) show the accumulation of protocatechuic acid from all three pigments, and of the pC-sophorose isomers and coumarin *p*-coumaroylglycoside from P1 and P4 (as after addition of 1 equiv. H_2O_2).

Interestingly, none of the P4 degradation products bears the sinapoyl residue (except traces of diacylsophorose). Again, the Sp residue is not only more prone to intramolecular migration than the pC residue, but also more labile or more reactive.

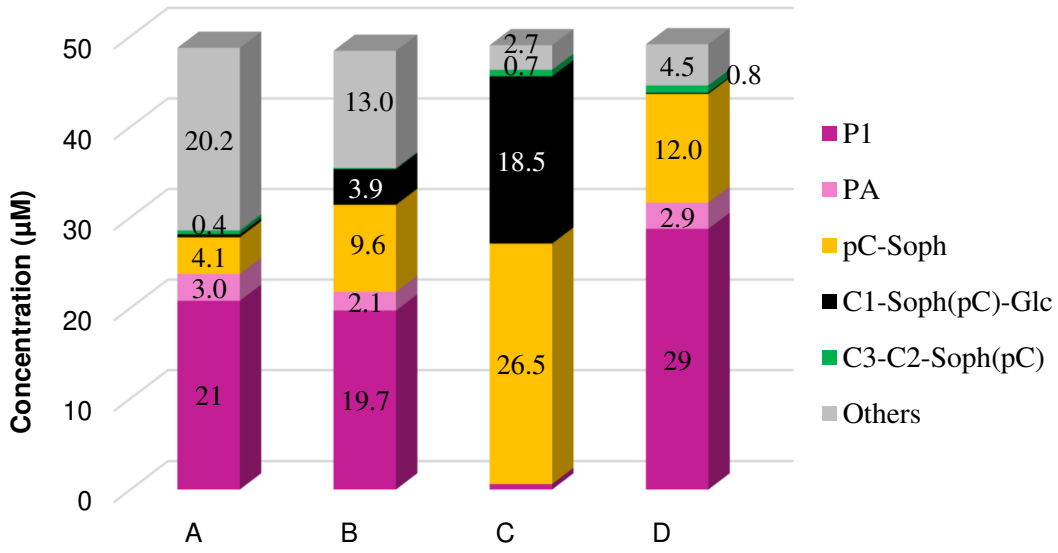

Fig. 4. Distribution of degradation products from P1 after 24h at pH 7, 50°C. **A:** P1. **B-C:** Impact of added H_2O_2 (**B:** 1 equiv., **C:** 10^3 equiv.), **D:** Impact of an argon atmosphere.

4. Discussion

At neutral pH, anthocyanins are a mixture of neutral and anionic bases slowly evolving into a mixture of hemiketal and chalcones. Upon moderate heating in neutral solution, red cabbage anthocyanins evolve by acyl hydrolysis and intramolecular transfer. The migration of the sinapoyl group (at C2-OH of Glc-2) appears specific to an acyl residue borne by a secondary C-atom. It is proposed to shift to the primary C-atom (C6-OH, major isomer) through the 2 intermediate secondary C-atoms (C3-OH and C4-OH, minor isomers). As most acylated anthocyanins display their acyl groups at primary C-atoms, this type of isomerization is generally not observed and constitutes a remarkable feature of red cabbage anthocyanins. Interestingly, when these anthocyanins are bound to iron, the sinapoyl residue loses its

410 mobility. The well-known propensity of HCA residues for developing π-stacking interactions
411 with the anthocyanidin nucleus [1,2] could be intensified within these complexes, given the
412 capacity of iron to coordinate up to 3 anthocyanin ligands [28], thereby increasing the rigidity
413 of the HCA residues and inhibiting their migration.

414 For red cabbage anthocyanins, the rate of anthocyanin consumption (oxidative
415 degradation) in neutral solution is not significantly different for the di- and monoacylated
416 pigments, and unexpectedly slightly faster than for the nonacylated one [6]. This observation
417 was interpreted by assuming that PA is rapidly converted into the colorless forms (by
418 reversible water addition), which are much more resistant to autoxidation than the electron-
419 rich anionic base (far more abundant in solutions of acylated anthocyanins) [6].

420 Upon degradation of an extract of purple sweet potato containing acylated 3-O-
421 sophorosyl-5-O-glucosylpeonidins (caffeoyl, feruloyl and *p*-hydroxybenzoyl residues), the
422 monoacylated anthocyanins appeared more stable than the diacylated ones [29]. However,
423 part of this apparent stability could be due to the partial hydrolysis of diacylated anthocyanins,
424 thereby replenishing the pool of monoacylated anthocyanins.

425 We recently showed that Fe^{2+} addition strongly slows down the rate of color loss in P4
426 solution at pH 7, mostly because the *p*-quinonemethide structure of P4 in the complex does
427 not undergo water addition [6]. This is consistent with Fe^{2+} addition inhibiting the formation
428 of the *trans*-chalcone. Besides its strong influence on the reversible color loss, Fe^{2+} addition
429 caused a modest slowing down of the early stage (up to 10h at pH 7, 50°C) of irreversible
430 degradation for P4, while the opposite holds for PA and P1 [6]. This difference was ascribed
431 to the higher stability of the iron – P4 (*vs.* iron – P1) complex due to enhanced π-stacking
432 interactions, while leakage of iron from the iron – P1 complex probably accelerates
433 autoxidation. However, 24h after iron addition, no protection of P4 against irreversible
434 degradation could be evidenced (Table 2). On the other hand, the accumulation of oxidation
435 products in iron-supplemented solutions obviously remains more modest in P4 than in P1
436 solution (Fig. 10-SI).

437 Our recent kinetic analysis suggests that the colored forms are primarily involved in the
438 oxidative degradation at pH 7 [6], which is consistent with the anionic base being probably a
439 much better electron donor than the other (neutral) species. We thus assume that the first step

consists in an electron transfer from A^- to O_2 under the mediation of transition metal traces, most probably Fe^{2+}. The aryloxyl radical thus formed can evolve through 2 distinct pathways (Scheme 3):

a) A second electron transfer to form a highly electrophilic *o*-quinone intermediate (pathway specific to B-rings having a 3',4'-dihydroxy substitution such as cyanidin derivatives) with concomitant generation of H_2O_2. Then, the *o*-quinone is expected to add a water molecule, thereby leading to intermediate I1.

b) Addition of O_2 with formation of a highly reactive peroxyl radical, which will rapidly abstract a labile H-atom from a second anthocyanin molecule, thus yielding intermediate I2, a hydroperoxide.

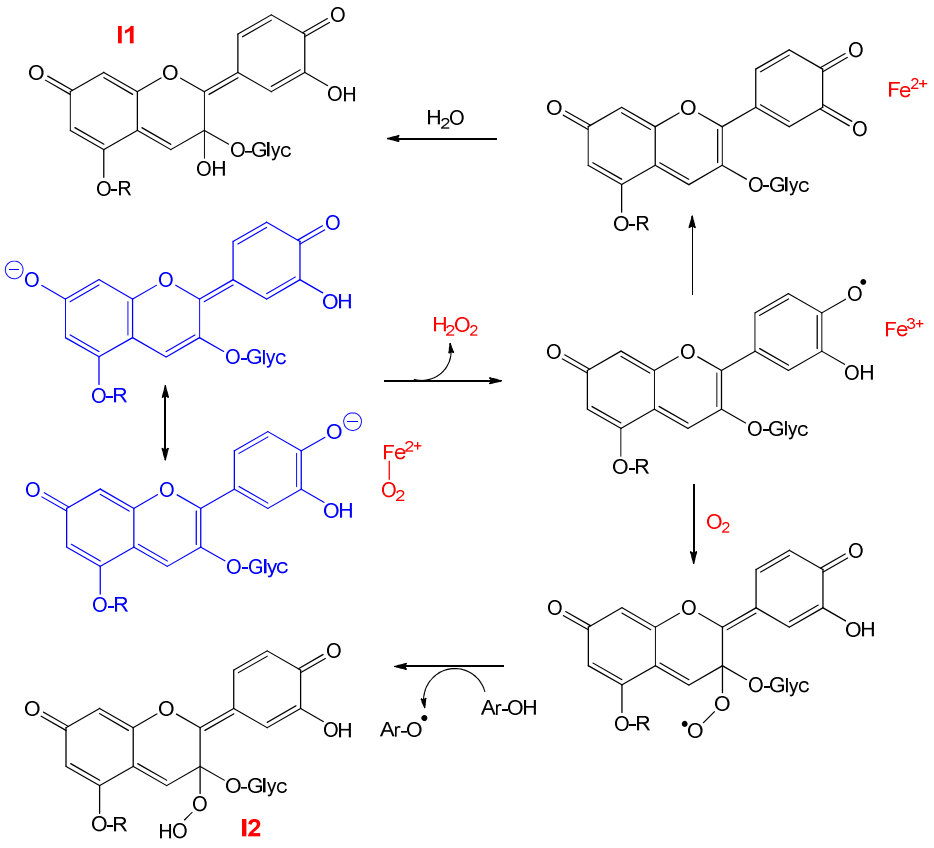

Scheme 3. Proposed mechanisms for the early stages of anthocyanin autoxidation in neutral solution.

Intermediates I1 and I2 may have different fates, some leading to products identified in this work or in the literature. In particular, I1 can add a second water molecule and form an intermediate already postulated to result from the electrophilic attack of H_2O_2 to the hemiketal in acidic solution [15]. From this intermediate, two end-products (belonging to the C3-C2 and C5 groups) duly identified by NMR can be produced (Scheme 4). Alternatively, elimination of the glycosyl group at C3-OH is feasible. More generally, the conversion of the glycosidic bond at C3-OH into an ester bond opens up a route for the release of the glycosyl group in neutral solution through simple hydrolysis.

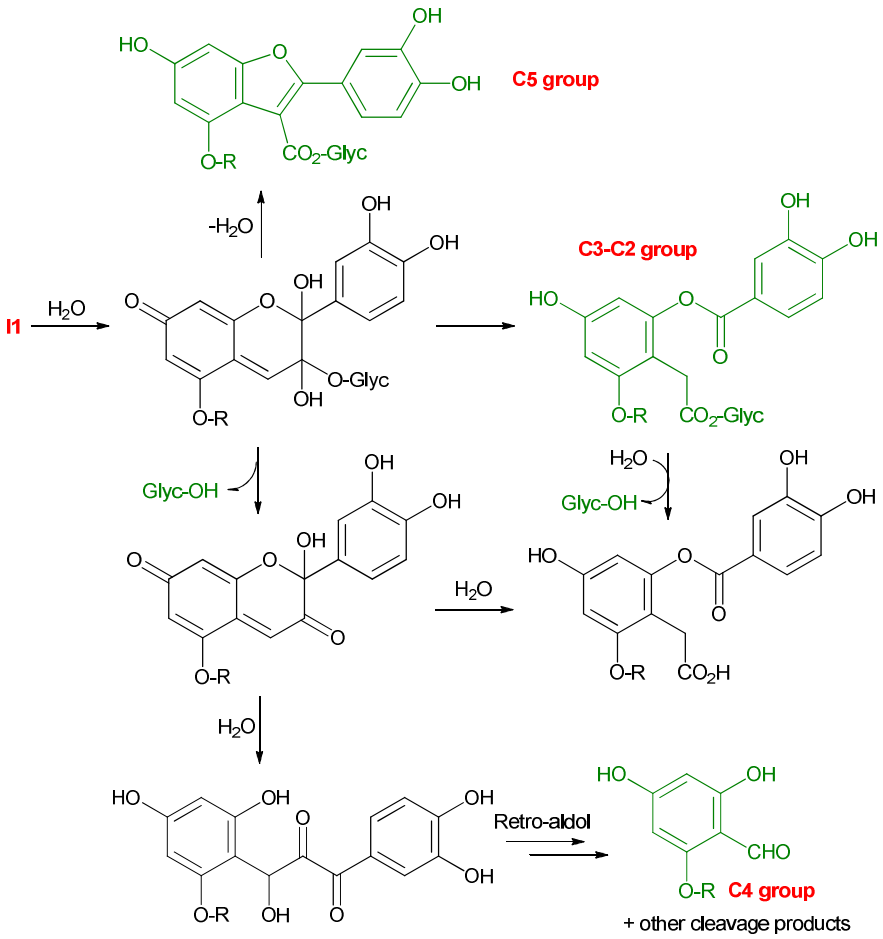

Scheme 4. Proposed mechanisms for the fate of intermediate I1.

Similar mechanisms can be written from I2 (Scheme 5). In this case, C3-C2 compounds are also expected, although in a two-electron oxidized version. Such a compound (two (*Z*,*E*) isomers) was indeed fully identified by NMR in the autoxidation of malvidin 3-O-glucoside in

acidic solution [25]. With a malvidin derivative (no catechol ring), the two-electron oxidation pathway is quenched and O_2 addition is actually the most likely fate for the aryloxyl radical. However, with the cyanidin derivatives investigated in this work, only the reduced version was evidenced, an indication that the two-electron oxidation pathway is privileged (Schemes 3 & 4) and/or that H_2O_2 addition to the anthocyanins also occurs (see below). Alternatively, formation of a 1,2-dioxetane ring (with concomitant re-aromatization of the A-ring) might open up a route for the formation of C4 derivatives (Scheme 5). Phloroglucinaldehyde and its glycosides are actually classical markers of anthocyanin degradation [10,11]. They could be formed by other routes, such as H_2O_2 addition to C3ox (free acid), followed by decarboxylation, or retro-aldol condensation from C-ring-opened intermediates (Scheme 4).

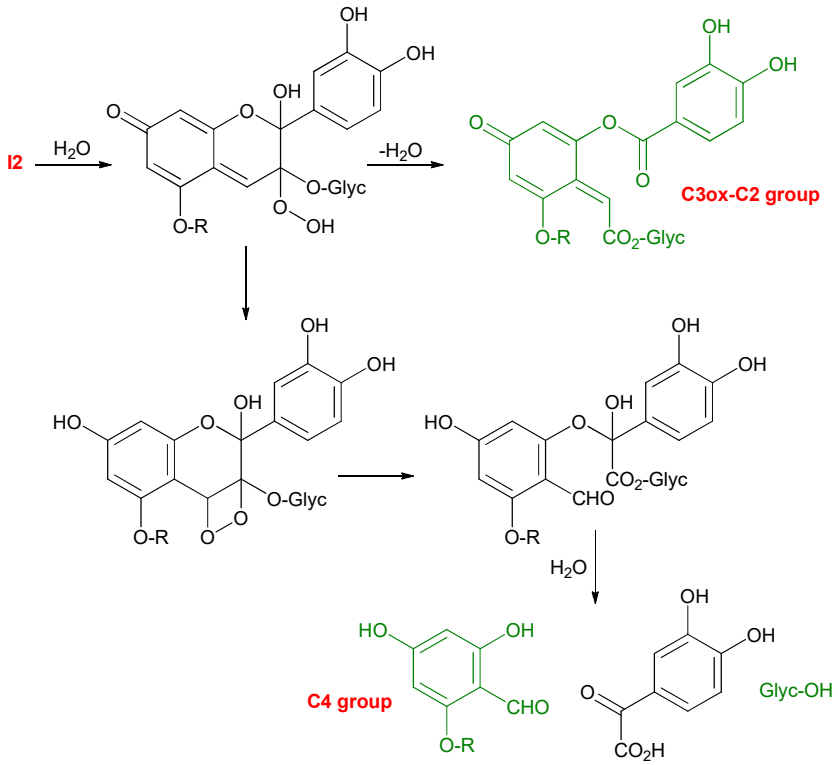

Scheme 5. Proposed mechanisms for the fate of intermediate I2.

Hydrogen peroxide produced in the autoxidation step probably participates in the oxidative degradation (as suggested by the experiments with added H_2O_2), either by electrophilic attack onto the anionic base or hemiketal (C3 position), or by nucleophilic attack onto the flavylium ion (C2 position) or chalcone (Bayer-Villiger reaction). The first route has

been convincingly demonstrated in acidic solution from labelling experiments (reaction with $H_2{}^{18}O_2$ or in $H_2{}^{18}O$) [15]. It leads to intermediate I1 (also produced by two-electron oxidation and subsequent water addition, Scheme 3) or its water adduct. The second route has the additional advantage to rationalize the formation of the coumarin derivatives. On the one hand, these products are detected at pH 5 – 7 but not at pH < 3 [23], which is not consistent with a mechanism involving the flavylium ion. On the other hand, addition of H_2O_2 indeed promotes their formation, *e.g.* **4'** (Fig. 4). Overall, the second route remains possible, although coumarins might be also produced through autoxidation of the anionic base (Scheme 3-SI). However, complementary products derived from the B-ring (*p*-hydroquinones in the Bayer-Villiger rearrangement, *p*-quinones in the autoxidation route) were not detected.

Finally, no direct participation of the HCA residues in the oxidative degradation could be evidenced and analyses by UPLC-DAD-MS and by capillary zone electrophoresis failed to detect anthocyanin dimers or higher oligomers.

5. Conclusions

Under the conditions where anthocyanins express blue colors, *i.e.* pH 7 in the presence of metal ions or pH 8, they undergo oxidative and hydrolytic pathways that alter the color and restrict their applications. The irreversible degradation of acylated red cabbage anthocyanins at 50°C leads to several groups of products, among which phloroglucinaldehyde-2-glucoside, *p*-coumaroylsophorose (a mixture of regioisomers) and derivatives of 2-(3,4-dihydroxy)benzoyloxy-4,6-dihydroxyphenylacetic acid are the major ones. Overall, the acylglycosides (*p*-coumaroylsophorose in this work) appear particularly stable and thus constitute suitable markers of the irreversible degradation of acylated anthocyanins.

In addition, the diacylated red cabbage anthocyanins appear remarkably prone to isomerization by intramolecular acyl transfer, a phenomenon that is evidenced for the first time.

Overall, the irreversible degradation of anthocyanins in neutral solution is probably kinetically controlled by an initial step of one- or two-electron autoxidation of the anionic base. The major oxidation products are thus proposed to derive either from the oxidized

anionic base itself or from an electrophilic attack of H_2O_2 (produced in the autoxidation step) to the anionic base.

For the development of anthocyanin extracts as food colorants in neutral media, the priority should be set at providing protection against autoxidation, for instance by the formation of stable redox-inert metal complexes or by adding suitable antioxidants.

Acknowledgements

The HRMS analyses were carried out on the ESI-Q-trap of the *Metaboscope* Platform funded by the European Fund for Regional Development, the French Ministry of Research, Higher Education and Innovation, the Region Provence-Alpes-Côte d'Azur, the Departmental Council of Vaucluse and the Urban Community of Avignon. The authors gratefully thank Christian Ginies for his support in the MS analyses, and Dr. Véronique Cheynier for helpful discussion.

References

[1] Trouillas P, Sancho-García JC, De Freitas V, Gierschner J, Otyepka M, Dangles O. Stabilizing and Modulating Color by Copigmentation: Insights from Theory and Experiment. Chem Rev 2016;116:4937–82. https://doi.org/10.1021/acs.chemrev.5b00507.

[2] Dangles O, Fenger J-A. The Chemical Reactivity of Anthocyanins and Its Consequences in Food Science and Nutrition. Molecules 2018;23:1970. https://doi.org/10.3390/molecules23081970.

[3] Moloney M, Robbins RJ, Collins TM, Kondo T, Yoshida K, Dangles O. Red cabbage anthocyanins: The influence of d-glucose acylation by hydroxycinnamic acids on their structural transformations in acidic to mildly alkaline conditions and on the resulting color. Dyes and Pigments 2018;158:342–52. https://doi.org/10.1016/j.dyepig.2018.05.057.

[4] Fenger J-A, Moloney M, Robbins RJ, Collins TM, Dangles O. The influence of acylation, metal binding and natural antioxidants on the thermal stability of red cabbage anthocyanins in neutral solution. Food Funct 2019;10:6740–51. https://doi.org/10.1039/C9FO01884K.

[5] Sigurdson GT, Robbins RJ, Collins TM, Giusti MM. Effects of hydroxycinnamic acids on blue color expression of cyanidin derivatives and their metal chelates. Food Chemistry 2017;234:131–

543 8. https://doi.org/10.1016/j.foodchem.2017.04.127.

544 [6] Cabrita L, Petrov V, Pina F. On the thermal degradation of anthocyanidins: cyanidin. RSC
545 Adv 2014;4:18939–44. https://doi.org/10.1039/C3RA47809B.

546 [7] Es-Safi N-E, Meudec E, Bouchut C, Fulcrand H, Ducrot P-H, Herbette G, et al. New
547 Compounds Obtained by Evolution and Oxidation of Malvidin 3- *O* -Glucoside in Ethanolic Medium.
548 Journal of Agricultural and Food Chemistry 2008;56:4584–91. https://doi.org/10.1021/jf8001872.

549 [8] Fleschhut J, Kratzer F, Rechkemmer G, Kulling SE. Stability and biotransformation of various
550 dietary anthocyanins in vitro. European Journal of Nutrition 2006;45:7–18.
551 https://doi.org/10.1007/s00394-005-0557-8.

552 [9] Sadilova E, Carle R, Stintzing FC. Thermal degradation of anthocyanins and its impact on
553 color and in vitro antioxidant capacity. Molecular Nutrition & Food Research 2007;51:1461–71.
554 https://doi.org/10.1002/mnfr.200700179.

555 [10] Seeram NP, Bourquin LD, Nair MG. Degradation Products of Cyanidin Glycosides from Tart
556 Cherries and Their Bioactivities. Journal of Agricultural and Food Chemistry 2001;49:4924–9.
557 https://doi.org/10.1021/jf0107508.

558 [11] Sinela A, Rawat N, Mertz C, Achir N, Fulcrand H, Dornier M. Anthocyanins degradation
559 during storage of Hibiscus sabdariffa extract and evolution of its degradation products. Food
560 Chemistry 2017;214:234–41. https://doi.org/10.1016/j.foodchem.2016.07.071.

561 [12] Stebbins NB. Ascorbic acid-catalyzed degradation of cyanidin-3- O-β-glucoside: Proposed
562 mechanism and identification of a novel hydroxylated product. Journal of Berry Research 2016;6:175–
563 87. https://doi.org/10.3233/JBR-160132.

564 [13] Satake R, Yanase E. Mechanistic studies of hydrogen-peroxide-mediated anthocyanin
565 oxidation. Tetrahedron 2018;74:6187–91. https://doi.org/10.1016/j.tet.2018.09.012.

566 [14] Pina F. Chemical Applications of Anthocyanins and Related Compounds. A Source of
567 Bioinspiration. Journal of Agricultural and Food Chemistry 2014;62:6885–97.
568 https://doi.org/10.1021/jf404869m.

569 [15] Mendoza J, Basílio N, Pina F, Kondo T, Yoshida K. Rationalizing the Color in Heavenly Blue
570 Anthocyanin. A Complete Kinetic and Thermodynamic Study. J Phys Chem B 2018;122:4982–92.
571 https://doi.org/10.1021/acs.jpcb.8b01136.

572 [16] Buchweitz M, Brauch J, Carle R, Kammerer DR. Colour and stability assessment of blue
573 ferric anthocyanin chelates in liquid pectin-stabilised model systems. Food Chemistry 2013;138:2026–

574 35. https://doi.org/10.1016/j.foodchem.2012.10.090.

575 [17] Ahmadiani N, Robbins RJ, Collins TM, Giusti MM. Molar absorptivity (ε) and spectral
576 characteristics of cyanidin-based anthocyanins from red cabbage. Food Chemistry 2016;197:900–6.
577 https://doi.org/10.1016/j.foodchem.2015.11.032.

578 [18] Preston NW, Timberlake CF. Separation of anthocyanin by high-performance liquid
579 chromatography. Journal of Chromatography 1981:222–8.

580 [19] Thévenet S, Wernicke A, Belniak S, Descotes G, Bouchu A, Queneau Y. Esterification of
581 unprotected sucrose with acid chlorides in aqueous medium: kinetic reactivity versus acyl- or
582 alkyloxycarbonyl-group migrations. Carbohydrate Research 1999;318:52–66.
583 https://doi.org/10.1016/S0008-6215(99)00079-8.

584 [20] Wiczkowski W, Szawara-Nowak D, Topolska J. Changes in the content and composition of
585 anthocyanins in red cabbage and its antioxidant capacity during fermentation, storage and stewing.
586 Food Chemistry 2015;167:115–23. https://doi.org/10.1016/j.foodchem.2014.06.087.

587 [21] Hrazdina G, Franzese AJ. Oxidation products of acylated anthocyanins under acidic and
588 neutral conditions. Phytochemistry 1974;13:231–4. https://doi.org/10.1016/S0031-9422(00)91300-1.

589 [22] Kamiya H, Yanase E, Nakatsuka S. Novel oxidation products of cyanidin 3-O-glucoside with
590 2,2′-azobis-(2,4-dimethyl)valeronitrile and evaluation of anthocyanin content and its oxidation in
591 black rice. Food Chemistry 2014;155:221–6. https://doi.org/10.1016/j.foodchem.2014.01.077.

592 [23] Lopes P, Richard T, Saucier C, Teissedre P-L, Monti J-P, Glories Y. Anthocyanone A: A
593 Quinone Methide Derivative Resulting from Malvidin 3-O-Glucoside Degradation. J Agric Food
594 Chem 2007;55:2698–704. https://doi.org/10.1021/jf062875o.

595 [24] Terahara N, Matsui T, Minoda K, Nasu K, Kikuchi R, Fukui K, et al. Functional New
596 Acylated Sophoroses and Deglucosylated Anthocyanins in a Fermented Red Vinegar. J Agric Food
597 Chem 2009;57:8331–8. https://doi.org/10.1021/jf901809p.

598 [25] Piffaut B, Kader F, Girardin M, Metche M. Comparative degradation pathways of malvidin
599 3,5-diglucoside after enzymatic and thermal treatments. Food Chemistry 1994;50:115–20.
600 https://doi.org/10.1016/0308-8146(94)90106-6.

601 [26] Estévez L, Sánchez-Lozano M, Mosquera RA. Complexation of common metal cations by
602 cyanins: Binding affinity and molecular structure. International Journal of Quantum Chemistry
603 2019;119:1–11. https://doi.org/10.1002/qua.25834.

604 [27] Xu J, Su X, Lim S, Griffin J, Carey E, Katz B, et al. Characterisation and stability of

605 anthocyanins in purple-fleshed sweet potato P40. Food Chemistry 2015;186:90–6.
606 https://doi.org/10.1016/j.foodchem.2014.08.123.

607